THE JOURNAL OF BIOLOGICAL CHEMISTRY VOL. 283, NO. 30, pp. 21054–21064, July 25, 2008

Identification of Farnesyl Pyrophosphate and *N*-Arachidonylglycine as Endogenous Ligands for GPR92*[S]

Received for publication, October 29, 2007, and in revised form, May 21, 2008 Published, JBC Papers in Press, May 22, 2008, DOI 10.1074/jbc.M708908200

Da Young Oh[‡], Jung Min Yoon[‡], Mi Jin Moon[‡], Jong-Ik Hwang[‡], Han Choe[§], Ju Yeon Lee[¶], Jae Il Kim[¶], Sunoh Kim[‖], Hyewhon Rhim[**], David K. O'Dell[‡‡], J. Michael Walker[†‡‡], Heung Sik Na[§§], Min Goo Lee[§§], Hyuk Bang Kwon[¶¶], Kyungjin Kim[‖‖], and Jae Young Seong[‡1]

From the [‡]Laboratory of G Protein-Coupled Receptors and [§§]Department of Physiology, Korea University College of Medicine, Seoul 136-705, Korea, the [§]Department of Physiology and Research Institute for Biomacromolecules, University of Ulsan College of Medicine, Seoul 138-736, Korea, the [¶]Department of Life Science, Gwangju Institute of Science and Technology, Gwangju 500-712, Korea, the [‖]Bio-Safety Research Institute and College of Veterinary Medicine, Chonbuk National University, Jeonju 561-756, Korea, the [**]Life Sciences Division, Korea Institute of Science and Technology, Seoul 136-791, Korea, the [‡‡]Gill Center for Biomolecular Science and Program in Neuroscience, Indiana University, Bloomington, Indiana 47405, the [¶¶]School of Biological Sciences and Technology, Chonnam National University, Gwangju 500-757, Korea, and the [‖‖]School of Biological Sciences, Seoul National University, Seoul 151-742, Republic of Korea

A series of small compounds acting at the orphan G protein-coupled receptor GPR92 were screened using a signaling pathway-specific reporter assay system. Lipid-derived molecules including farnesyl pyrophosphate (FPP), *N*-arachidonylglycine (NAG), and lysophosphatidic acid were found to activate GPR92. FPP and lysophosphatidic acid were able to activate both $G_{q/11}$- and G_s-mediated signaling pathways, whereas NAG activated only the $G_{q/11}$-mediated signaling pathway. Computer-simulated modeling combined with site-directed mutagenesis of GPR92 indicated that Thr^{97}, Gly^{98}, Phe^{101}, and Arg^{267} of GPR92 are responsible for the interaction of GPR92 with FPP and NAG. Reverse transcription-PCR analysis revealed that GPR92 mRNA is highly expressed in the dorsal root ganglia (DRG) but faint in other brain regions. Peripheral tissues including, spleen, stomach, small intestine, and kidney also expressed GPR92 mRNA. Immunohistochemical analysis revealed that GPR92 is largely co-localized with TRPV1, a nonspecific cation channel that responds to noxious heat, in mouse and human DRG. FPP and NAG increased intracellular Ca^{2+} levels in cultured DRG neurons. These results suggest that FPP and NAG play a role in the sensory nervous system through activation of GPR92.

G protein-coupled receptors (GPCRs)[2] are the largest family of cell surface receptors and play a wide variety of roles in pathophysiological processes by transmitting extracellular signals to cells via heterotrimeric G proteins. Many members of this superfamily are major targets of pharmaceutical drugs (1). Completion of the human genome project revealed the structures of many novel GPCRs for which the natural ligands remain to be identified, so-called orphan GPCRs. Because identification of the ligands for orphan GPCRs is important for understanding the physiological roles of these receptors and promises a rich source of potential drug candidates, efforts have been made to identify the ligands of these receptors (2–4).

The human *GPR92* (also known as *GPR93*) gene was first discovered by customized GenBank™ searches (5). It is located on chromosome 12, region p 13.31 and contains two noncoding and coding exons encoding 372 amino acid residues (6). GPR92 belongs to the rhodopsin-like GPCR family and is structurally related to GPR23/LPA_4 receptor, an atypical lysophosphatidic acid (LPA) receptor that shares only 20–24% amino acid identity with conventional LPA receptors (LPA_{1-3}) (7). This structural relationship led to an identification of LPA as a GPR92 ligand (6, 8). LPA increased cAMP levels and inositol phosphate (IP) production and induced intracellular calcium mobilization in cells expressing GPR92. This indicates that GPR92 is likely coupled to G_s and $G_{q/11}$. Further LPA-induced neurite retraction and stress fiber formation in GPR92-expressing cells suggests that GPR92 is also coupled to $G_{12/13}$ (6).

This LPA responsiveness of GPR92 along with its structural similarity to LPA_4 led to the suggestion that this receptor be renamed the LPA_5 receptor (6). It should be noted, however,

* This work was supported, in whole or in part, by National Institutes of Health Grants DA16825 and DA018224 from the National Institute on Drug Abuse (to J. M. W.). This work was also supported by Grants M103KV010005-08K2201-00510 (to J. Y. S.) and M103KV010007-07K2201-00710 (to H. R.) from the Brain Research Center of the 21st Century Frontier Research Program; the Linda and Jack Gill Center for Biomolecular Science, Indiana University, Bloomington, IN; and the Indiana Metabolomics and Cytomics Initiative (METACyt) Grant from Lilly Foundation Inc., Indianapolis, IN. The costs of publication of this article were defrayed in part by the payment of page charges. This article must therefore be hereby marked "*advertisement*" in accordance with 18 U.S.C. Section 1734 solely to indicate this fact.
This paper is dedicated to the memory of J. Michael Walker.
[S] The on-line version of this article (available at http://www.jbc.org) contains supplemental Figs. 1–4.
† Passed away on January 5, 2008 in Bloomington, IN.
[1] To whom correspondence and reprint requests should be addressed. Tel.: 82-2-920-6090; Fax: 82-2-921-4355; E-mail: jyseong@korea.ac.kr.

[2] The abbreviations used are: GPCR, G protein-coupled receptor; FPP, farnesyl pyrophosphate; NAG, *N*-arachidonylglycine; DRG, dorsal root ganglia; IP, inositol phosphate; GFP, green fluorescent protein; LPA, lysophosphatidic acid; m.o.i., multiplicity of infection; GTPγS, guanosine 5′-*O*-3-thiotriphosphate; SRE, serum response element; luc, luciferase; HEK293, human embryonic kidney 293; 2-AG, 2-arachidonoyl glycerol; DMEM, Dulbecco's modified Eagle's medium; ERK, extracellular signal-regulated kinase; MAPK, mitogen-activated protein kinase; NF200, neurofilament 200 kDa; CCD, charge-coupled device; siRNA, small interfering RNA; CRE, cAMP-responsive element.

that GPR92 has only a 35% amino acid homology with the LPA_4 receptor. Additionally EC_{50} values for various LPA compounds in the production of cAMP and IP in GPR92-expressing cells range between 0.5 and 5 μM. This indicates that LPA is a moderately potent activator of GPR92 (6, 8). More recently, a luminal protein hydrolysate was found to activate GPR92 and possess a higher potency for cAMP production than LPA (9). These findings suggest the possibility that molecules other than LPA can serve as ligands for GPR92 and that perhaps reference to this compound as the LPA_5 receptor would be premature.

While searching for orphan GPCR ligands using various chemical compounds, we found that many lipid-derived molecules are able to activate GPR92 with different potencies. Of these, farnesyl pyrophosphate (FPP) was more potent than LPA in activating GPR92 as revealed by E_{max} and EC_{50} values. *N*-Arachidonylglycine (NAG) was as potent as LPA in activation of GPR92. FPP and LPA activated both G_s- and $G_{q/11}$-linked signaling pathways, whereas NAG was able to activate only the $G_{q/11}$-linked signaling pathway. Using computer-simulated molecular modeling combined with site-directed mutagenesis, we identified amino acid residues responsible for the interaction of GPR92 with FPP and NAG. Reverse transcription-PCR analysis revealed that GPR92 mRNA was present in high levels in the dorsal root ganglia (DRG) in the nervous system as well as in the spleen, stomach, intestine, and kidney. Further FPP and NAG induced Ca^{2+} mobilization in cultured DRG cells.

EXPERIMENTAL PROCEDURES

Chemicals—The chemicals 12-*O*-tetradecanoylphorbol-13-acetate and FPP were purchased from Sigma. U73122 and MDL-12330A were obtained from Calbiochem. We obtained 2-arachidonoyl glycerol (2-AG) from Cayman Chemical (Ann Arbor, MI). LPA (14:0) was purchased from Avanti Polar Lipids (Alabaster, AL). All acylamides, including NAG, *N*-arachidonyl γ-aminobutyric acid, *N*-palmitoylserine phosphoric acid, *N*-arachidonylalanine, and *N*-arachidonylserine, were synthesized as described previously (10).

Plasmids—The cDNA for human GPR92 was constructed at HindIII and XbaI sites of pcDNA3, whereas cDNA for mouse GPR92 was constructed at EcoRI and XhoI of pcDNA3 (Invitrogen). Site-directed mutagenesis of human GPR92 was generated by the PCR overlapping extension method (11). All PCR-derived sequences were verified by automatic sequencing. pCMV β-Gal was purchased from Clontech. SRE-luc, containing a single copy of the serum response element (SRE; CCATATTAGG) followed by a c-*fos* basic promoter and luciferase, was constructed. Adenoviruses containing human GPR92 or an SRE-luc reporter were obtained from Neugex Co. (Seoul, Korea).

Adenovirus Infection, Transfection, and Luciferase Assay—Adenovirus infection and luciferase assays were performed as described previously (4). CV-1 cells were maintained in DMEM in the presence of 10% fetal bovine serum. Cells (5×10^3) were plated into a 96-well plate. Cells were coinfected with adenoviruses containing human GPR92 and an SRE-luc reporter with 50 multiplicity of infection (m.o.i.) under serum-free conditions for 3 h. Cells were then incubated with 10% fetal bovine serum-containing DMEM.

For SRE-luc analysis, cells were maintained in serum-free DMEM for at least 16 h before treatment. Following treatment of cells with an agonist for 6 h, cells were harvested. Luciferase activity in the cell extracts was determined according to standard methods using a Wallac 1420 VICTOR^3 plate reader (PerkinElmer Life Sciences). For transfection of GPR92 mutants, CV-1 cells were plated into 24-well plates and transfected 24 h later with Effectene reagent (Qiagen, Valencia, CA). The total amount of DNA used in each transfection was adjusted to 1 μg by adding appropriate amounts of pcDNA3. Forty-eight hours after transfection, cells were treated with ligands for 6 h.

GTPγS Binding Assay—Forty-eight hours after infection of CV-1 cells with adenoviruses containing human GPR92 or vehicle, cells were homogenized in 5 mM Tris-HCl, 2 mM EDTA (pH 7.4) and centrifuged at 48,000 × *g* for 15 min at 4 °C. The resulting pellets were washed in 50 mM Tris-HCl, 10 mM $MgCl_2$ (pH 7.4) and stored at −80 °C until use. Agonist-stimulated [^{35}S]GTPγS binding was determined as described previously (12). Briefly membrane fractions (15 μg) were incubated for 15 min at room temperature in binding buffer (20 mM HEPES (pH 7.4), 100 mM NaCl, 3 mM $MgCl_2$, and 3 μM GDP) in the presence of various concentrations of FPP, LPA, or NAG. [^{35}S]GTPγS (0.2 nM) was added. Then samples were further incubated for 30 min at 30 °C. The incubation was stopped by centrifugation at 1000 × *g* for 10 min at 4 °C. Bound GTPγ[^{35}S] was counted in a scintillation mixture. Nonspecific binding was determined in the presence of 10 μM GTPγS to be less than 10% of total binding.

Measurement of Inositol Phosphate Production—An IP production assay was performed as described previously (13). CV-1 cells were seeded into a 12-well plate and infected with adenoviruses containing human GPR92 with 100 m.o.i. After infection, cells were incubated in M199 medium (Invitrogen) in the presence of 1 μCi/ml *myo*-[^{3}H]inositol (Amersham Biosciences)/well for 20 h. Medium was removed, and cells were washed with 0.5 ml Buffer A (140 mM NaCl, 20 mM HEPES, 4 mM KCl, 8 mM D-glucose, 1 mM $MgCl_2$, 1 mM $CaCl_2$, and 1 mg/ml fatty acid-free bovine serum albumin). Cells were then preincubated for 30 min with Buffer A containing 10 mM LiCl followed by addition of 1 μM FPP, 10 μM NAG, or 10 μM LPA at 37 °C for 30 min with or without 15-min prior treatment with a phospholipase C inhibitor, U73122. Replacing incubation medium with 0.5 ml of ice-cold 10 mM formic acid terminated the reaction. After 30 min at 4 °C, the formic acid extracts were transferred to columns containing Dowex anion-exchange resin (AG-1-X8 resin, Bio-Rad). Total IPs were then eluted with 1 ml of ammonium formate, 0.1 M formic acid. Radioactivity was determined using a Tri-Carb 3100TR scintillation counter (PerkinElmer Life Sciences).

cAMP Assay—Cyclic AMP levels were determined by measuring [^{3}H]cAMP formation from [^{3}H]ATP (13). Twenty-four hours before transfection, HeLa cells were seeded into 12-well plates. Cells were transfected with the pcDNA3-GPR92 plasmid with Effectene reagent. One day later, cells were labeled with 2 μCi/ml [^{3}H]adenine (PerkinElmer Life Sciences) for

24 h. Cells were first washed in phosphate-buffered saline and then incubated at 37 °C for 20 min in serum-free DMEM containing 1 mM 1-methyl-3-isobutylxanthine. Cells were stimulated with 1 μM FPP, 10 μM NAG, or 10 μM LPA for 30 min with or without 15-min prior treatment with an adenylate cyclase inhibitor, MDL-12330A. The reactions were terminated by replacing the medium with ice-cold 5% trichloroacetic acid containing 1 mM ATP and 1 mM cAMP. [^{3}H]cAMP and [^{3}H]ATP were separated on AG 50W-X4 resin (Bio-Rad) and alumina columns as described previously (13). The cAMP accumulation was expressed as [^{3}H]cAMP/([^{3}H]ATP + [^{3}H]cAMP) × 1000.

Ca^{2+} Mobilization Assay—F11 rat embryonic neuroblastoma × DRG neuron hybrid cells (generous gifts from Dr. Henning Otto, Freie Universität, Berlin, Germany) were transiently transfected with hGPR92-GFP and grown on poly-D-lysine-coated glass coverslips for 24–48 h. Cells were then incubated in a physiological solution (138 mM NaCl, 6 mM KCl, 1 mM $MgSO_4$, 2 mM $CaCl_2$, 1 mM Na_2HPO_4, 5 mM $NaHCO_3$, 5 mM glucose, 10 mM HEPES, and 0.1% bovine serum albumin) with 5 μM fura-2/AM (Molecular Probes, Eugene, OR) at room temperature for 45 min. Cells were washed twice with the dye-free physiological solution and mounted in an acrylamide chamber that allows for perfusion of incubation medium. Fura-2/AM fluorescence was measured in GFP-positive cells at excitation wavelengths 340 and 380 nm and at emission wavelength 510 nm using an IX70 fluorescence microscope (Olympus, Tokyo, Japan) coupled to a digital cooled CCD camera (CoolSNAP fx CCD camera, Roper Scientific, Tucson, AZ).

ERK Activation—CV-1 cells (2×10^5) were plated on a 60-mm dish for 1 day before infection with adenoviruses containing GPR92. Cells were infected with 100 m.o.i. adenoviruses for 3 h in serum-free DMEM. Then the medium was changed to 10% fetal bovine serum-containing DMEM. Before protein preparation for ERK Western blotting, cells were incubated for at least 16 h in serum-free medium prior to agonist stimulation. After agonist stimulation in the presence or absence of 100 ng/ml pertussis toxin, cells were lysed by RIPA buffer (50 mM Tris HCl (pH 8.0), 150 mM NaCl, 1% Nonidet P-40, 0.1% SDS, 1 mM EDTA, and protease inhibitor mixture) followed by boiling at 95 °C for 5 min. Equal amounts of cellular extracts were separated on 10% polyacrylamide gels and transferred to nitrocellulose membranes for immunoblotting. Phosphorylated ERK1/2 and total ERK1/2 were detected by immunoblotting with mouse monoclonal anti-phospho-p44/42 MAPK (Cell Signaling Technology, 1:2000) and anti-p44/42 MAPK (Cell Signaling Technology, 1:2000), respectively. Chemiluminescence detection was performed using the ECL reagent.

Molecular Modeling—A homology model of GPR92 was built on the basis of the 2.2-Å crystal structure (Protein Data Bank code 1U19) of the bovine rhodopsin (14) using the homology modeling program molIDE (15). Hydrogen atoms and Kollman-all charges were added to the homology model of GPR92 using Sybyl v7.0 (Tripos Inc., St. Louis, MO). The three-dimensional structure of FPP and NAG was sketched and refined using the Sybyl program with the Gasteiger-Huckel charge method. The virtual docking of clomipramine was performed using GOLD v3.0, a program that applies stochastic genetic algorithms for conformational searching (16). The number of genetic operations was set to 1×10^5, and the population size was set to 1×10^2. All structural figures were prepared using PyMol v0.98 (DeLano Scientific LLC, San Francisco, CA).

Reverse Transcription-PCR Analysis—Total RNA was isolated from mouse tissues using TRI Reagent (Sigma). Two micrograms of total RNA were reverse transcribed with Moloney murine leukemia virus reverse transcriptase (Invitrogen) according to the manufacturer's instructions. The cDNA was amplified by PCR using the following primers: mGPR92-F (5′-TGGCAGAGTCTTCTGGACACT-3′; 681–701) and mGPR92-R (5′-GCCAAAGGCCTGGTTTCAGCG-3′; 989–1010). The PCR cycling parameters were as follows: denaturation at 95 °C for 5 min followed by 35 cycles of denaturation at 95 °C for 30 s, annealing at 57.5 °C for 30 s, and extension at 72 °C for 45 s. PCR products were separated on a 1.5% agarose gel, stained with ethidium bromide, and photographed under a UV light source.

Immunocytochemistry and Histochemistry—The mouse lumbar DRG was isolated from 6-week-old male C57B/6 mice. The human DRG was isolated from fresh cadavers with the informed consent of the relatives of body donors and the approval of the ethics committee of the Korea University College of Medicine, Seoul, Korea. The isolated DRG was fixed for 4 h in 4% paraformaldehyde, washed with 1× phosphate-buffered saline, and cryoprotected overnight in 30% sucrose. The DRG was serially cut (10 μm) on a cryostat and mounted on gelatin-coated slides. Slides were incubated in 1× phosphate-buffered saline containing 5% bovine serum albumin and 0.1% Triton X-100 for 1 h at room temperature. Sections were incubated overnight in primary antibody at 4 °C and washed three times with 1× phosphate-buffered saline. The primary antibodies used in this study are as follows: mouse GPR92 (1:100, MBL International, Woburn, MA), human GPR92 (1:1000, Abcam), mouse and human TRPV1 (1:1000, Abcam), and neurofilament 200 kDa (NF200; 1:1000, Chemicon, Temecula, CA). After several washes, sections were incubated with fluorescence-labeled secondary antibodies (anti-rabbit-Alexa594 antibody for human and mouse GPR92, anti-guinea pig-Alexa488 antibody for TRPV1, and anti-mouse-Alexa488 antibody for NF200, Molecular Probes), and nuclei were counterstained with Hoechst33342 (10

TABLE 1

Agonistic potency to induce SRE-luc activity in CV-1 cells expressing GPR92

CV-1 cells were infected with 50 m.o.i. adenovirus with GPR92 in combination with 50 m.o.i. adenovirus with SRE-luc. Luciferase assays were examined after ligand stimulation for 6 h. Each value represents the mean ± S.E. of three independent experiments performed in triplicate. NAA, *N*-arachidonylalanine; NAS, *N*-arachidonylserine; NAGABA, *N*-arachidonyl γ-aminobutyric acid; NPSPA, *N*-palmitoylserine phosphoric acid.

Ligand	EC_{50}	E_{max}
	μM	*-fold induction over basal*
FPP	0.26 ± 0.08	28.79 ± 1.46
NAG	4.47 ± 0.73	8.20 ± 0.38
LPA	1.82 ± 0.73	8.76 ± 0.79
NAA	>10	
NAS	>10	
NAGABA	3.79 ± 1.34	4.15 ± 0.26
2-AG	1.78 ± 0.63	9.04 ± 1.21
NPSPA	7.33 ± 2.87	3.92 ± 0.27

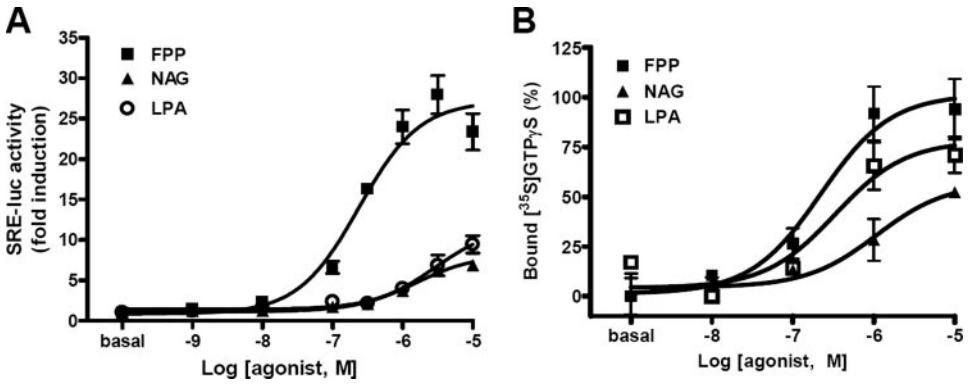

FIGURE 1. **Response of GPR92 to FPP and NAG.** *A*, CV-1 cells were coinfected with adenoviruses containing human GPR92 and SRE-luc in 96-well plates. Forty-eight hours after infection, cells were treated with the indicated concentration of FPP, NAG, or LPA for 6 h. Cells were harvested, and luciferase activities in the cell extracts were measured. The results are plotted as -fold activity over basal activity. Each *bar* represents means ± S.E. of three independent experiments performed in triplicate. *B*, FPP-, NAG-, and LPA-induced [^{35}S]GTPγS binding to membrane fractions of CV-1 cells infected with adenoviruses containing GPR92. [^{35}S]GTPγS binding was determined in a binding buffer containing 100 μM GDP in the presence of various concentrations of FPP, LPA, and NAG. The increase in [^{35}S]GTPγS binding is indicated as the percentage of specific binding to basal binding. Data are expressed as mean ± S.E.

TABLE 2

EC_{50} and E_{max} of IP and cAMP production by FPP, NAG, and LPA in GPR92-expressing cells

CV-1 cells were infected with 100 m.o.i. adenovirus with human GPR92 and stimulated with different concentrations of FPP, NAG, and LPA in 12-well plates. IP and cAMP assays were performed as described under "Experimental Procedures." Data are expressed as the mean ± S.E. of three independent experiments performed in triplicate assays. The E_{max} values for NAG and LPA are -fold induction at 10 μM.

Ligands	IP production		cAMP production	
	EC_{50}	E_{max}	EC_{50}	E_{max}
	μM		μM	
FPP	0.38 ± 0.15	4.41 ± 0.56	1.46 ± 0.52	3.15 ± 0.22
NAG	>50	2.01 ± 0.25		
LPA	1.03 ± 0.42	2.98 ± 0.19	>50	2.44 ± 0.30

μg/ml) for 30 min at room temperature. Fluorescence labeling was observed under an LSM510 confocal laser microscope (Zeiss). Images were optimized for quantification using Adobe Photoshop 7.0 (Adobe Systems, San Jose, CA).

DRG Cultures and Intracellular Ca^{2+} Imaging—Cultured DRG neurons were prepared using a technique modified from Rhim *et al.* (17). Briefly DRG were isolated from all levels of the lumbar and sacral spinal cord from Sprague-Dawley rats (100–150 g) and incubated with 0.15% collagenase (Sigma) for 20 min and then with 0.125% trypsin (Sigma) for 10 min in Ca^{2+}- and Mg^{2+}-free HEPES buffer solution at 37 °C. DRG neurons were then mechanically dissociated with Pasteur pipettes by trituration and plated on poly-L-lysine-coated coverslips. Cells were maintained in DMEM supplemented with 10% fetal bovine serum, 1 mM sodium pyruvate, 100 units/ml penicillin, and 100 μg/ml streptomycin under a humidified atmosphere of 95% air, 5% CO_2 at 37 °C. For intracellular Ca^{2+} imaging recordings, cells were used within 1–2 days after plating. The diameter of each DRG neuron was defined as the average of the distance along the longest and shortest axis of the cell body. All chemicals used for cell preparation were purchased from Invitrogen. For intracellular Ca^{2+} imaging, the acetoxymethyl ester form of fura-2 (fura-2/AM, Molecular Probes) was used as the fluorescent Ca^{2+} indicator. DRG neurons were incubated for 60 min at room temperature with 5 μM fura-2/AM and 0.001% Pluronic F-127 in a HEPES-buffered solution composed of 150 mM NaCl, 5 mM KCl, 1 mM $MgCl_2$, 2.5 mM $CaCl_2$, 10 mM HEPES, and 10 mM glucose (pH adjusted to 7.4 with NaOH). Cells were then washed with HEPES-buffered solution and placed on an inverted microscope (Olympus). Cells were illuminated using a xenon arc lamp. The required excitation wavelengths (340 and 380 nm) were selected with a computer-controlled filter wheel (Sutter Instruments, Novato, CA). Emitter fluorescence light was reflected through a 515-nm long pass filter to a frame transfer cooled CCD camera. The ratios of emitted fluorescence were calculated using a digital fluorescence analyzer. All imaging data were collected and analyzed using Meta Imaging Software (Molecular Devices Corp., Downingtown, PA).

Cell Transfection—DRG cells were transfected after 1 day in culture using Lipofectamine 2000. Briefly GPR92 siRNA (5′-CGUUUGCAUAUGGUGUdTdT-3′) or a nontargeting scrambled siRNA (negative) and the Lipofectamine 2000 diluted in serum-free DMEM/F-12 were combined and incubated at room temperature for 20 min. After the culture media were removed and saved, cells were incubated with the siRNA/Lipofectamine 2000 mixture at 37 °C for 4 h. Cells were then incubated with the saved culture media for 48 h. To monitor transfection efficiency, the GFP expression vector pEGFP-N1 (Clontech) was co-transfected with each siRNA. For each Ca^{2+} imaging experiment, the transfected cells without the GFP vector were loaded with fura-2/AM after separately confirming transfection efficiency (>80%).

Data Analysis—All assays were performed in triplicate and repeated three times. The data are presented as mean ± S.E. of at least three independent experiments. Data analysis was performed using nonlinear regression. Data are expressed using sigmoidal dose-response curves. Agonist concentrations inducing half-maximal stimulation (EC_{50}) and maximal -fold increase (E_{max}) were calculated using the GraphPad PRISM4 software (GraphPad, San Diego, CA). One-way analysis of variance followed by Newman-Keuls post-test was used for data analyses. $p < 0.05$ was considered statistically significant.

RESULTS

Ligand Screening for GPR92—We previously established a widely applicable screening system to identify ligands for orphan GPCRs (4). In this system, cDNAs for orphan GPCR and GPCR signaling-specific reporter genes are introduced to adenovirus. These reporter genes include a cAMP-responsive element-driven luciferase gene (CRE-luc) for G_s- and $G_{i/o}$-linked pathways and SRE-luc for $G_{q/11}$- or $G_{12/13}$-linked pathways (4, 13). We screened ligands for GPR92 using CV-1 cells that were doubly infected by adenoviruses containing human

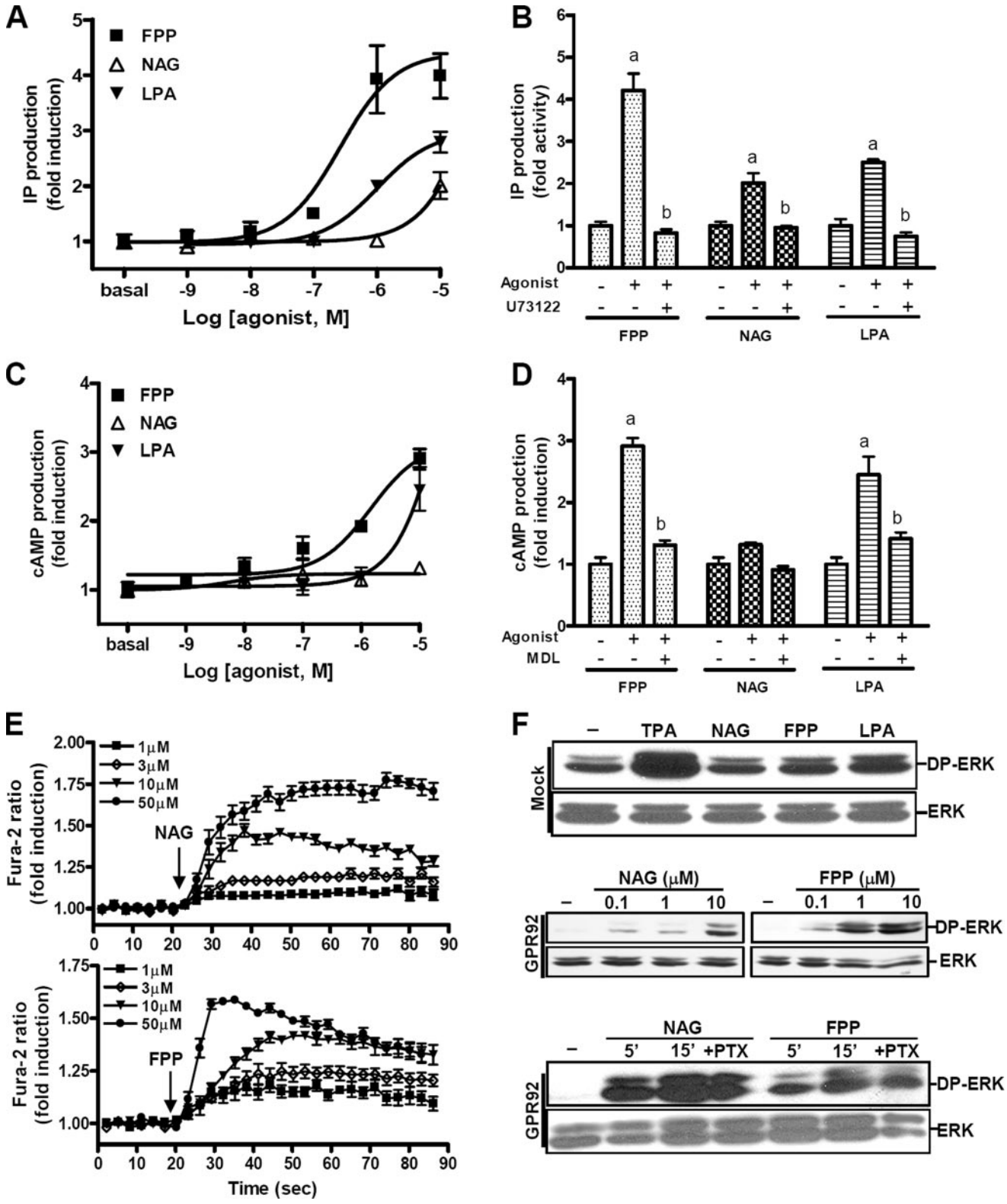

FIGURE 2. **GPR92-mediated signaling pathways.** *A* and *C*, IP production (*A*) or cAMP accumulation (*C*) in response to various concentrations of FPP, NAG, or LPA were determined in CV-1 cells infected with adenoviruses containing GPR92. *B* and *D*, the specificity of the signaling pathway was verified by pretreating with U73122 (10 μM), a phospholipase C inhibitor (*B*), and MDL-12330A (10 μM), an adenylate cyclase inhibitor (*C*), 15 min before treatment with 10 μM FPP, NAG, or LPA, respectively. *a*, $p < 0.05$ *versus* the control group (basal); *b*, $p < 0.05$ *versus* the agonist-stimulated group. *E*, effects of FPP and NAG on intracellular Ca^{2+} levels in GPR92-expressing cells were examined. Increased intracellular Ca^{2+} was found in F11 cells transiently expressing GPR92-GFP. Cells were treated with various concentration of FPP and NAG. *F*, ERK1/2 activation by agonists in GPR92-infected cells. CV-1 cells were infected with 100 m.o.i. adenoviruses with GPR92 and were serum-starved for 16 h prior to agonist stimulation. The mock-infected cells (*F*, *upper panel*) were treated with 1 μM FPP, 10 μM of NAG and LPA, and 200 nM 12-*O*-tetradecanoylphorbol-13-acetate (*TPA*) as a positive control for 5 min. GPR92-infected CV-1 cells (*F*, *middle panel*) were treated with various concentrations of NAG and FPP. Involvement of G_i activation in ERK1/2 phosphorylation was determined by pretreatment with 100 ng/ml pertussis toxin (*PTX*) (*F*, *bottom panel*). *DP*, double phosphorylated. The *prime* represents minutes. Data are expressed as the mean ± S.E. of three independent experiments.

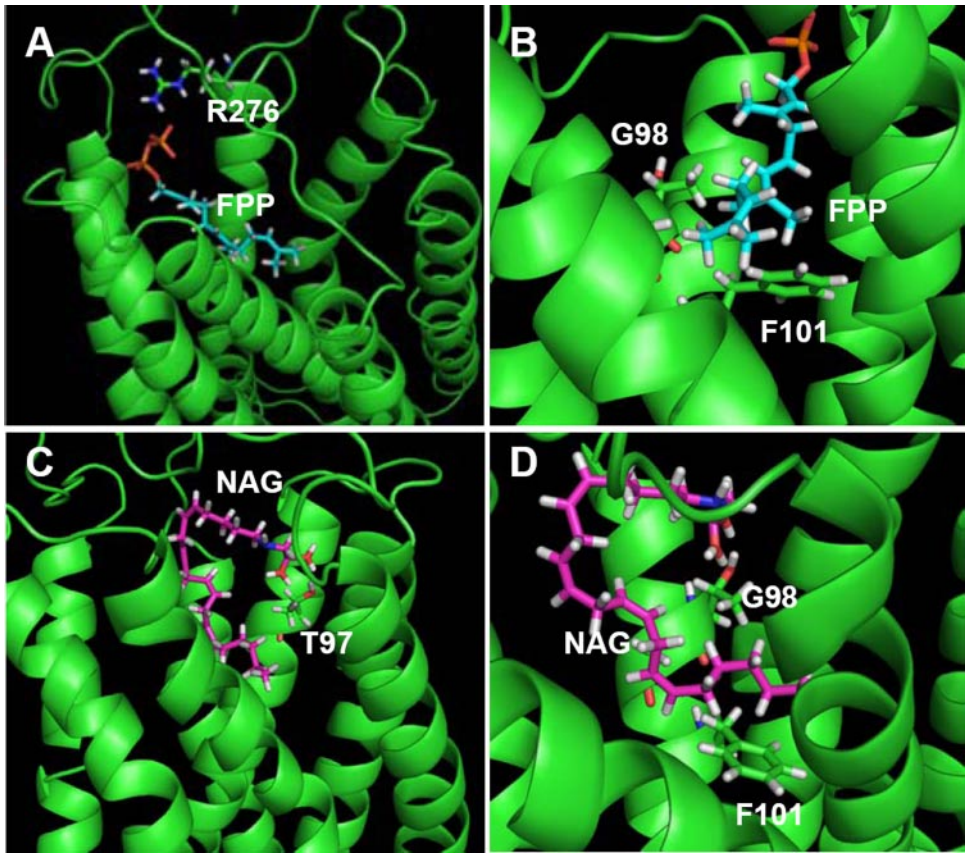

FIGURE 3. **Molecular docking of FPP or NAG to GPR92.** GPR92 and ligands were drawn as *ribbon* and *stick* models, respectively. Transmembrane domains of GPR92 are drawn as *ribbons* in *green*. Interacting residues of GPR92 are also drawn as a *stick* model in the following colors: carbon atoms in *green*, nitrogen atoms in *deep blue*, hydrogen atoms in *gray*, and oxygen atoms in *red*. For FPP and NAG, carbon atoms are in *sky blue* and *purple*, respectively. The phosphate, oxygen, nitrogen, and hydrogen atoms are in *orange*, *red*, *deep blue*, and *gray*, respectively. *A*, the positively charged side chain of Arg^{276} electrostatically interacts with the negatively charged diphosphate moiety of FPP. *B*, Gly^{98} and Phe^{101} of GPR92 have close contacts with the hydrophobic carbon chain of FPP. *C*, Thr^{97} interacts with the glycine moiety of NAG. *D*, the hydrophobic carbon chain of NAG contacts Gly^{98} and Phe^{11} of GPR92.

TABLE 3

EC_{50} and E_{max} values of FPP and NAG for wild type and mutant GPR92

The plasmids containing the wild type and mutant human GPR92 were cotransfected with the SRE-luc reporter vector into CV-1 cells along with β-galactosidase as an internal control. Forty-eight hours after transfection, cells were treated with graded concentrations of FPP and NAG for 6 h, and luciferase activity was determined. NR, no response to ligands. Each value represents the mean ± S.E. of three independent experiments performed in triplicate.

Receptor	EC_{50}		E_{max}	
	FPP	NAG	FPP	NAG
	μM		*-fold induction over basal*	
Wild type	0.21 ± 0.05	1.52 ± 0.23	26.90 ± 1.17	8.21 ± 0.38
T97I	0.21 ± 0.10	>10	30.00 ± 3.23	4.28 ± 0.23
T97L	0.50 ± 0.16	>10	26.61 ± 2.07	3.09 ± 0.13
T97A	0.62 ± 0.24	>10	27.01 ± 2.97	3.82 ± 0.53
G98F	NR	NR	NR	NR
G98K	NR	NR	NR	NR
G98A	0.24 ± 0.08	>10	11.62 ± 0.82	2.92 ± 0.06
F101W	1.60 ± 0.38	NR	27.57 ± 2.09	NR
F101A	0.33 ± 0.10	4.41 ± 1.89	30.26 ± 1.84	8.95 ± 1.21
R276S	NR	2.03 ± 0.87	NR	6.14 ± 0.75
R276K	>10	2.57 ± 0.86	27.34 ± 5.74	7.47 ± 0.83
R276A	NR	NR	NR	NR

GPR92 and SRE-luc or CRE-luc. Cells were treated with various lipid-derived molecules. GPR92 activity was determined by measuring luciferase activity.

In an initial screening, FPP, NAG, LPA, 2-AG, *N*-arachidonyl γ-aminobutyric acid, *N*-palmitoylserine phosphoric acid, *N*-arachidonylalanine, and *N*-arachidonylserine were found to activate GPR92. Dose-response studies showed that FPP had the highest potency with an EC_{50} of 0.26 μM, approximately 10 times lower than that of LPA (Fig. 1*A*). NAG, 2-AG, *N*-arachidonyl γ-aminobutyric acid, and LPA showed EC_{50} values ranging from 2 to 5 μM (Table 1). Further FPP showed 3-fold higher efficacy than other lipid-derived molecules.

To examine whether the agonist-induced SRE-luc activity is mediated by G protein coupling, a [^{35}S]GTPγS binding assay was performed using cells expressing GPR92 in the presence of various concentrations of FPP, LPA, or NAG. FPP dose-dependently increased [^{35}S]GTPγS binding to cell fractions containing GPR92 with a higher potency than NAG and LPA (Fig. 1*B*). No agonist-induced increases in [^{35}S]GTPγS binding were observed in mock-infected cells.

Signaling Pathways of GPR92—To investigate the signaling pathways of GPR92, we determined the levels of various second messengers after treatment with FPP, NAG, or LPA. Treatment of GPR92-expressing cells with these agonists resulted in a concentration-dependent increase in IP production. FPP showed the highest potency for IP production followed by LPA and NAG (Fig. 2*A* and Table 2). Agonist-induced production of IP was completely blocked by U73122, a phospholipase C inhibitor, indicating that GPR92 is G_q-coupled (Fig. 2*B*).

FPP and LPA, but not NAG, increased cAMP levels in a dose-dependent manner (Fig. 2*C* and Table 2). Agonist-induced increases in cAMP levels were suppressed by MDL-12330A, an adenylate cyclase inhibitor (Fig. 2*D*), indicating that GPR92 is able to couple with G_s. The -fold induction of IP and cAMP by FPP was higher than the induction levels produced by LPA and NAG. To further determine the involvement of a cAMP-linked pathway, we performed an additional experiment using a CRE-luc reporter. The cells were coinfected with adenovirus containing GPR92 and CRE-luc and treated with various concentrations of FPP, LPA, and NAG. FPP and LPA increased CRE-luc reporter activity, whereas NAG failed to do so (supplemental Fig. 1A). H89, a cAMP-dependent protein kinase inhibitor, was able to inhibit both FPP- and LPA-induced CRE-luc activity (supplemental Fig. 1B). This study again demonstrated the involvement of the cAMP/cAMP-dependent protein kinase pathway in GPR92-mediated signaling.

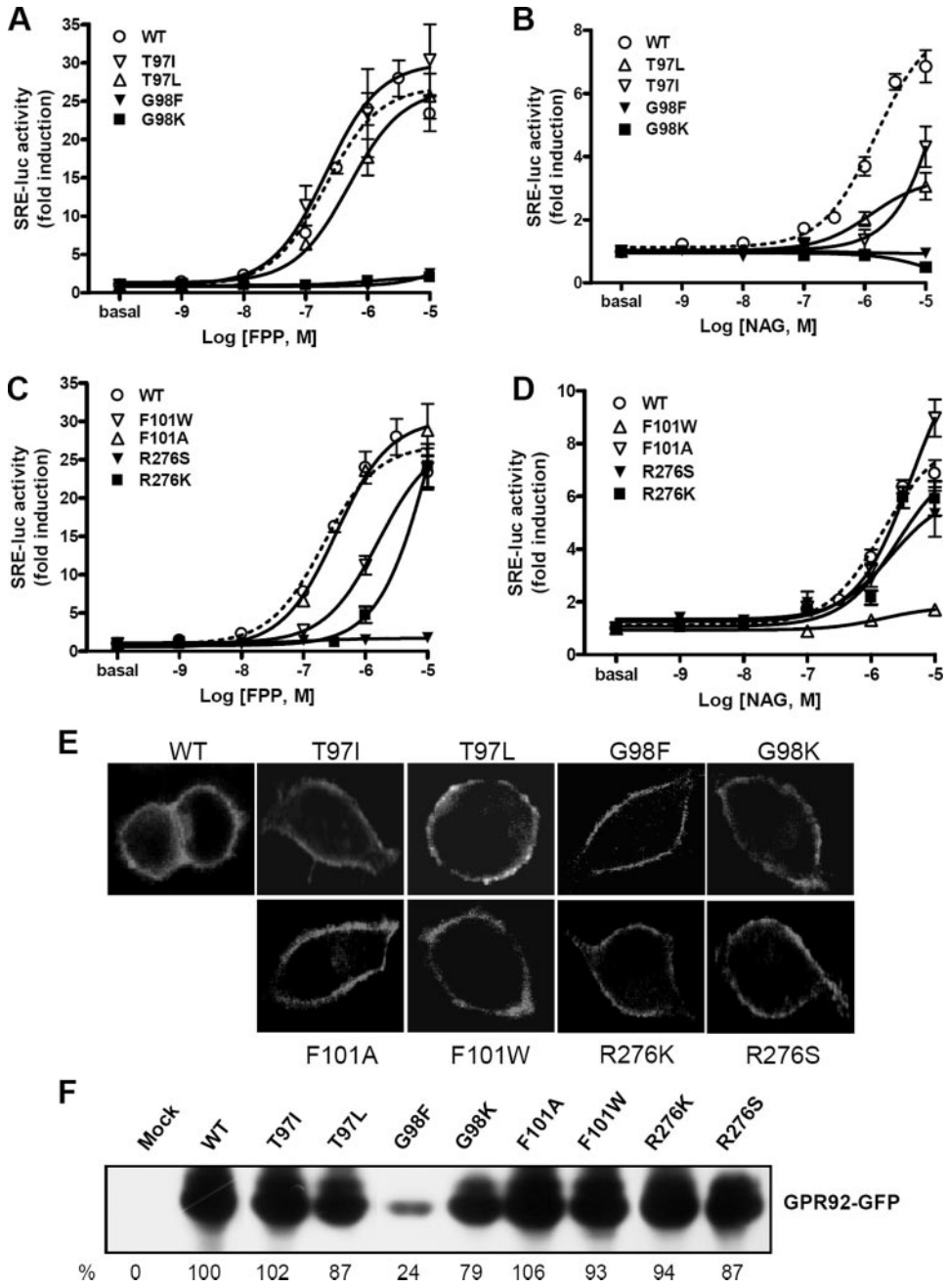

FIGURE 4. **Dose-response activities of wild type and mutant GPR92 stimulated by FPP or NAG.** Wild type (*WT*) and mutant GPR92 were co-transfected with SRE-luc in CV-1 cells. Cells were then treated with the indicated concentrations of FPP or NAG for 6 h. Luciferase activities were measured and normalized against β-galactosidase activity. The results are plotted as -fold activity over basal luciferase activity. SRE-luc activities of wild type and mutant receptors T97I, T97L, G98F, G98K (*A* and *B*), F101W, F101A, R276S, and R276K (*C* and *D*) in response to FPP (*A* and *C*) and NAG (*B* and *D*) are shown. Data represent means ± S.E. of three independent experiments performed in triplicate. *E*, subcellular localization of GFP-fused GPR92 mutants. HeLa cells were transfected with GFP-fused GRP92 mutants and serum-starved for 16 h. Fluorescence labeling was observed under a confocal laser microscope. *F*, protein expression levels of wild type and mutant GPR92-GFP were determined by Western blot using an anti-GFP antibody. Percent expression levels are presented as the mean of two independent experiments.

We then examined whether FPP and NAG can increase intracellular Ca^{2+} levels in GPR92-expressing cells. F11 cells transfected with GFP-fused human GPR92 were treated with various concentrations of FPP or NAG. Dose-dependent inductions of intracellular Ca^{2+} concentration were observed only in GFP-positive cells (Fig. 2*E*).

Treatment of cells with FPP or NAG for 5 min elevated phospho-ERK levels (Fig. 2*F*, *middle panel*), whereas these agonists did not elevate phospho-ERK levels beyond basal amounts in mock-infected cells. A slight increase in phospho-ERK levels by LPA in mock-infected cells is likely due to expression of other types of LPA receptors in these cells (Fig. 2*F*, *upper panel*). Increased phospho-ERK levels were maintained for 15 min. Increases were not blocked by pertussis toxin, a specific inhibitor of G_i (Fig. 2*F*, *lower panel*), indicating that the increase in phospho-ERK level is independent of G_i activation.

Identification of Ligand-binding Residues of GPR92—Although FPP and NAG have different chemical structures, they are able to activate the same receptor, which provided the impetus to investigate the ligand-binding residues of GPR92 used in binding to different agonists. To address this question, we constructed a molecular model of GPR92 based on the rhodopsin structure and performed a virtual docking of the ligands to the receptor to predict the putative binding sites of GPR92 for FPP and NAG. Molecular modeling results revealed that the negatively charged diphosphate moiety of FPP has an electrostatic interaction with Arg^{276} in the third extracellular loop of GPR92 (Fig. 3*A*). Gly^{98} and Phe^{101} at transmembrane domain 3 have close contacts with the hydrophobic carbon chain of FPP (Fig. 3*B*). As Gly has the smallest side chain, it may provide a space for docking of the hydrophobic carbon chain of FPP. The glycine moiety of NAG interacts with Thr^{97} at transmembrane domain 3 of GPR92 (Fig. 3*C*). Like FPP, the hydrophobic carbon chain of NAG has close contact with Gly^{98} and Phe^{101} (Fig. 3*D*).

Support for the modeling data was obtained by mutating these potential binding residues. EC_{50} and E_{max} values of FPP and NAG for wild type and mutant GPR92 are summarized in Table 3. Mutation of Thr^{97} to Ile (T97I), to Leu (T97L), and to Ala (T97A) significantly decreased response to NAG. However, these mutants responded to FPP with potency similar to that of the wild

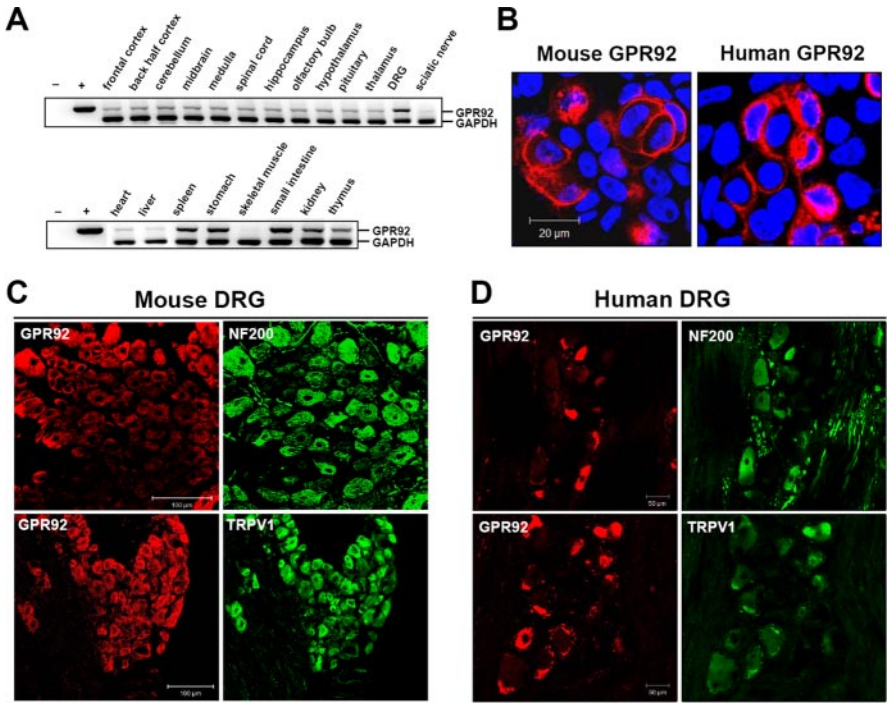

FIGURE 5. **Tissue distribution of GPR92 mRNA and immunohistochemistry of GRP92 in the mouse and human DRG.** *A*, total RNA levels from 6-week-old C57B/6 male mice in the indicated tissues were assessed by reverse transcription-PCR. Glyceraldehyde-3-phosphate dehydrogenase (*GAPDH*) was used as a loading control. *B* and *C*, for validation of the anti-GPR92 antibody, an immunofluorescence assay was performed in HeLa cells expressing mouse GPR92 and human GPR92. Mouse GPR92 and human GPR92 were detected using an anti-rabbit-Alexa594 secondary antibody and an LSM510 confocal microscope. *C* and *D*, immunohistochemistry of mouse (*C*) and human DRG (*D*) using anti-GPR92 in combination with anti-NF200 or anti-TRPV1 antibodies. *Scale bars* in *B–D* represent 20, 100, and 50 μm, respectively.

type receptor (Fig. 4, *A* and *B*), indicating that Thr^{97} might be important for NAG interaction. Mutation of Gly^{98} to Phe (G98F) or to Lys (G98K) completely abolished responsiveness to both FPP and NAG (Fig. 4, *A* and *B*). Mutation of Gly^{98} to Ala (G98A) also reduced responsiveness to both FPP and NAG (supplemental Fig. 2, A and B). This result indicates that the small Gly^{98} may be important for forming a binding pocket. A tight steric hindrance caused by the bulky side chains of Phe and Lys may hamper binding to both FPP and NAG.

Mutation of Phe^{101} to Trp (F101W) drastically decreased sensitivity to NAG, whereas it reduced sensitivity to FPP to a level 10-fold lower than wild type (Fig. 4, *C* and *D*). Mutation of Phe^{101} to Ala (F101A), however, did not change sensitivity to either NAG or FPP. Replacement of Arg^{276} with Ser (R276S) completely abolished the FPP response but resulted in retention of responsiveness to NAG. Lys substitution (R276K) significantly decreased sensitivity to FPP and NAG. This finding suggests that the positively charged side chain of Arg^{276} may participate in an electrostatic interaction with the negatively charged diphosphate group of FPP.

To examine whether reduced responsiveness of mutant receptors to agonists is due to aberrant surface expression of the receptor, the subcellular localization of GFP-fused mutant receptors was determined. Like the wild type receptor, all mutant receptors were localized to plasma membrane (Fig. 4*E*). Further we examined protein expression level by Western blot using an anti-GFP antibody, showing no remarkable differences in expression levels except for G98F (24% of wild type expression) (Fig. 4*F*). This result together with the membrane expression of mutant receptors suggests that reduced or complete loss of responsiveness to agonists is not mainly due to aberrant or reduced expression of the mutant except for G98F.

Expression Pattern of GPR92 in the Mouse Tissues and Human DRG—Regional distribution of GPR92 mRNA in the mouse brain and peripheral tissues was assessed by reverse transcription-PCR analysis (Fig. 5*A* and supplemental Fig. 3A). GPR92 mRNA was expressed broadly at low levels throughout the brain regions and was expressed at relatively high levels in the DRG, spleen, stomach, small intestine, kidney, and thymus. GPR92 protein expression was further evaluated by immunohistochemical staining. To examine whether antibodies for GPR92 were appropriate for immunohistochemistry, we first performed immunocytochemistry in cells expressing mouse or human GPR92. Antibodies for mouse and human GPR92 specifically recognized mouse and human GPR92, respectively (Fig. 5*B*).

For DRG immunohistochemistry, GPR92 was doubly stained with the neuronal markers NF200 and TRPV1 to distinguish subgroups of DRG neurons. In both mouse and human DRG, the anti-NF200 antibody recognized large diameter neurons, whereas TRPV1 mainly stained medium and small diameter neurons. In the mouse DRG, GPR92 was faintly labeled in NF200-negative cells, whereas some signals were observed in NF200-positive cells. GPR92 was strongly labeled in TRPV1-positive cells (Fig. 5*C*). In the human DRG, GPR92 was distributed in small diameter neurons but rarely detected in NF200-positive neurons (Fig. 5*D*). Double staining of human DRG sections with GPR92 and TRPV1 revealed that the majority of TRPV1-positive neurons also expressed GPR92 (Fig. 5*D*). No cross-activity between GPR92 and TRPV1 antibodies was observed (supplemental Fig. 3, B and C).

FPP and NAG-induced Ca^{2+} Mobilization in Cultured DRG Neurons—We next examined the function of GPR92 by treating cultured rat DRG neurons with FPP or NAG. Agonist-induced Ca^{2+} responses were mainly observed in small diameter neurons. Some neurons responded to both FPP (1 μM) and NAG (10 μM), whereas others responded to only FPP or NAG (Fig. 6, *A–D*). Of the small diameter neurons tested (diameter <30 μm, $n = 200$), 15% responded to FPP, NAG, and capsaicin. Additionally 10% responded to FPP and NAG but not to capsaicin. These FPP- or NAG-mediated Ca^{2+} increases were

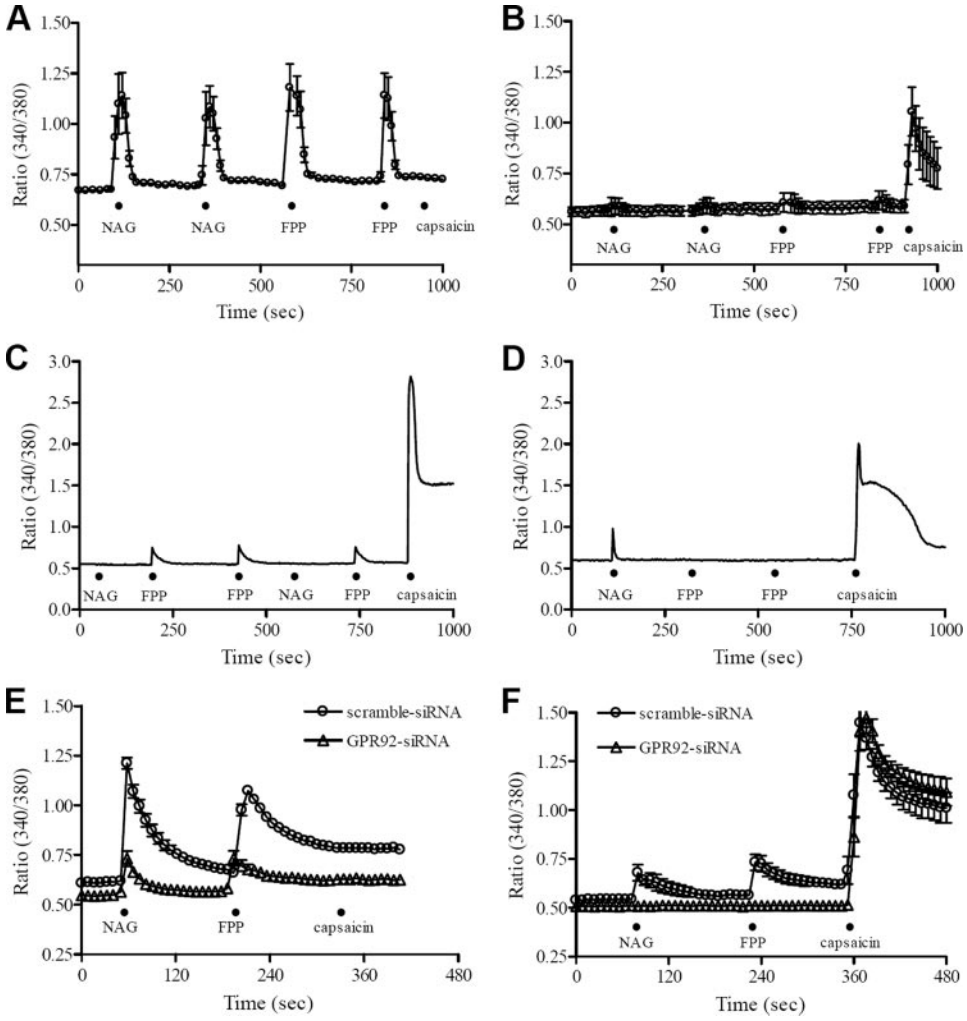

FIGURE 6. **FPP- and NAG-induced Ca^{2+} mobilization in cultured small DRG neurons.** A time course shows the effects of FPP and NAG on rat cultured DRG neurons using fura-2-based digital imaging techniques. The application of FPP (1 μM) or NAG (10 μM) for 10 s increased intracellular Ca^{2+} in HEPES-buffered solution (n = 5). *A* and *B* are pooled data obtained from five DRG neurons, whereas *C* and *D* are sampled recordings showing differential responses of FPP and NAG on a cultured DRG neuron. The *black dot* (●) represents acute application of each indicated drug. The response to capsaicin (0.1 μM) was examined in all DRG neurons tested. *E* and *F* are pooled data obtained from 12–27 siRNA-transfected DRG neurons. To knock down GPR92, cultured rat DRG neurons were exposed to siRNA against GPR92 (△). As a negative control siRNA (○), a nontargeting scrambled siRNA with no sequence homology to any known gene sequences was used. *E* and *F* represent agonist-induced $[Ca^{2+}]_i$ signals in capsaicin-insensitive and -sensitive cells, respectively.

repeatedly observed by second application of the agonist. However, treatment of medium (30–40 μm) or large (>40 μm) diameter DRG neurons with FPP or NAG did not produce any changes in Ca^{2+} responses. To confirm that these agonist-induced Ca^{2+} increases occur via an activation of GPR92, we used siRNA-mediated silencing of GPR92 in cultured rat DRG neurons. The selective knockdown of GPR92 was confirmed by Western blot analysis (supplemental Fig. 4A). To monitor transfection efficiency in cultured rat DRG neurons, the GFP expression vector pEGFP-N1 was co-transfected with each siRNA (supplemental Fig. 4B). For each Ca^{2+} imaging experiment, the transfected cells without the GFP vector were loaded with fura-2/AM after separately confirming transfection efficiency (>80%). Agonist-induced $[Ca^{2+}]_i$ increases were still observed in the scrambled siRNA-transfected cells. However, GPR92 siRNA-transfected cells showed much smaller $[Ca^{2+}]_i$ increases compared with scrambled siRNA-transfected cells. For capsaicin-insensitive cells, GPR92 knockdown resulted in a 68.2 ± 0.8 and 64.3 ± 1.3% inhibition of NAG- and FPP-mediated $[Ca^{2+}]_i$ increases, respectively (Fig. 6*E*). For capsaicin-sensitive cells, the NAG- and FPP-mediated $[Ca^{2+}]_i$ increases were completely inhibited in GPR92 knockdown cells (Fig. 6*F*).

DISCUSSION

Human GPR92 is structurally most closely related to GPR23/LPA_4, a recently identified receptor for LPA (7). Indeed GPR92 binds to LPA. This binding induces $G_{q/11}$-, $G_{12/13}$-, and G_s-mediated signaling pathways (6, 8). Because the EC_{50} value for LPA in the production of IP and cAMP in cells expressing GPR92 ranges in micromolar levels, there is likely to be an agonist that is more potent than LPA. This possibility was further supported by the observation that a luminal extract is more potent than LPA in inducing cAMP production in GPR92-expressing cells (8).

While searching for potential GPR92 agonists, we observed that GPR92 is activated by various lipid-derived molecules with different affinities. Of these molecules, FPP demonstrated a higher potency and efficacy for activating GPR92 than LPA. FPP showed an approximate 10-fold lower EC_{50} value and 3-fold higher E_{max} value than LPA in agonist-induced SRE-luc activity in cells expressing GPR92. NAG showed a potency similar to that of LPA for inducing SRE-luc activity.

One might suggest that FPP-induced SRE-luc activity is likely not due to G protein coupling because FPP can contribute to transcriptional activation independent of GPCR-mediated G protein activation. FPP is a donor for isoprenylation of many proteins, including the $\beta\gamma$ subunit of heterotrimeric G proteins and the small GTPases such as Ras and Rho. Isoprenylation is necessary for translocation of these G proteins to the plasma membrane and subsequent activation (18–20). Because SRE can possibly serve as a downstream target of FPP-mediated Ras activation, it can be postulated that FPP-induced SRE-luc activity in this study is due to Ras activation. Further FPP is found to be a novel transcriptional activator for a subset of nuclear hormone receptors (21), suggesting possible G protein-independent

effects of FPP on SRE-luc activity. However, this FPP-induced SRE-luc activity is only observed in GPR92-expressing cells but not in mock-infected cells. In GPR92-expressing cells, FPP induced immediate responses, such as Ca^{2+} mobilization, accumulation of IP and cAMP, and elevation of phospho-ERK. Additionally increased [^{35}S]GTPγS binding indicates that FPP may have a direct interaction with GPR92, leading to activation of a G protein such as G_s and $G_{q/11}$.

Most GPCRs respond to a single endogenous ligand. Some phylogenetically related receptors share a common ligand. However, some receptors respond to more than two different compounds, each with different affinities (2, 3). GPR92 responds to various lipid-derived molecules including FPP, NAG, and LPA. These compounds possess a long hydrophobic carbon chain with a polar moiety. Our molecular modeling study, combined with site-directed mutagenesis, revealed that hydrophobic moieties of FPP and NAG have common binding sites, Gly^{98} and Phe^{101}, at transmembrane domain 3. Gly^{98} is likely important for forming a binding pocket that allows a hydrophobic interaction between Phe^{101} of GPR92 and the hydrophobic carbon chains of FPP and NAG. In addition to common binding sites, GPR92 has specific binding residues for charged moieties of FPP and NAG. The negatively charged diphosphate moiety of FPP and the glycine moiety of NAG interact with Arg^{276} in the third extracellular loop and Thr^{97} at the transmembrane domain 3, respectively. In this regard, molecular interactions between GPR92 and other molecules such as LPA and 2-AG remain to be elucidated.

FPP and NAG are endogenously synthesized. FPP is a key intermediate in the biosynthesis of steroids, carotenoids, and polyisoprenoids. FPP is easily transported into plasma. The steady-state human plasma concentration of FPP is ~7 ng/ml (~15 nM) (22). As the mRNA for GPR92 is expressed in a variety of peripheral tissues, including spleen, thymus, stomach, small intestine, and kidney, it is possible that circulating FPP may exert its effects in these tissues through activation of GPR92.

NAG is naturally produced in a variety of tissues including the spinal cord, small intestine, kidney, glabrous skin, and brain (10). These tissues also contain GPR92 mRNA. Recently NAG was identified as an endogenous ligand for GPR18; it activates the G_i-mediated signaling pathway (23). This suggests that NAG plays a role in immune regulation because GPR18 is highly expressed in lymphoid tissues such as the peripheral blood leukocytes, spleen, and thymus (24, 25). The biological functions of NAG with regard to GPR92, however, are not yet understood. However, as tissue distributions of GPR92 and NAG are highly correlated (5, 10), it is postulated that NAG has a role in these tissues through activation of GPR92.

In good agreement with a previous observation (6), GPR92 was highly expressed in the DRG where FPP and NAG are able to induce Ca^{2+} elevation. This indicates possible roles of FPP and NAG in the DRG. FPP and its synthase activities are present in the spinal cord (26), suggesting a role of FPP in sensory neurotransmission through activation of GPR92. NAG is highly concentrated in the spinal cord and glabrous skin (10), which indicates a physical interaction of NAG with GPR92 in sensory neurons. However, it is not known how FPP and NAG are regulated in physiological conditions and whether FPP and NAG have direct actions on DRG neurons.

An interesting finding of this study is that GPR92 was expressed at high levels in small and medium diameter neurons of the DRG, which include primary sensory fibers associated with acute and neuropathic pain. Many GPR92-positive cells in the DRG coexpress TRPV1, which functions as a nociceptor (27). FPP- and NAG-induced Ca^{2+} elevation was observed only in small diameter DRG neurons. Some FPP- and NAG-responsive cells responded to capsaicin, a TRPV1 agonist. Of the capsaicin-responsive DRG neurons, ~38% of the cells responded to either FPP or NAG. This observation, together with coexpression of GPR92 and TRPV1, indicates a possible role of GPR92 in TRPV1-medicated pain sensing. Recently involvement of GPR92 in neuropathic pain has been suggested because GPR92 knock-out mice display significantly less sensitivity in the spinal cord to noxious mechanical and thermal stimulation than wild type littermates (28).

Several reports suggest involvement of NAG in nociception in the sensory nervous system. No evidence for the role of FPP in nociception has been provided. Peripheral administration of NAG in the hind paw is capable of suppressing the phase 2 response of formalin-induced pain behavior in the rat (10). Further recent studies suggest involvement of NAG in inflammatory and neuropathic pain. Intrathecal administration of NAG reduces the mechanical allodynia and thermal hyperalgesia induced by either intraplantar injection of Freund's complete adjuvant or partial ligation of the sciatic nerve (29, 30). NAG is a structural analog of the endogenous cannabinoid anandamide. However, the pain suppressive effects of NAG are not likely mediated by activation of the cannabinoid CB1 receptor because NAG has a very poor affinity to the CB1 receptor (31, 32). One possible explanation for the effects of NAG is that NAG increases anandamide concentration by inhibiting the hydrolytic activity of fatty acid amide hydrolase on anandamide (33). Alternatively the coexpression of GPR92 and TRPV1 in the DRG raises the possibility that NAG can exert its pain suppressive effects through GPR92 in the sensory nervous system. As NAG acts as a partial agonist at GPR92, it is possible that it serves as an antagonist to FPP under physiological conditions thereby reducing activation of GPR92, although this possibility should be further investigated.

In summary, we have demonstrated that multiple lipid-derived molecules can activate GPR92 with different potencies. Of these, FPP was by far the most potent ligand and exerted effects with much greater efficacy than any of the other compounds tested, including LPA. However, we do not exclude the possible presence of other, as yet unknown, GPR92 agonists that have even greater efficacy. The presence of multiple ligands for GPR92 portends a wide range of biological and medicinal roles for this receptor. The roles of FPP and NAG through activation of GPR92 in peripheral tissues and the DRG require further investigation.

REFERENCES

1. Wilson, S., and Bergsma, D. (2000) *Drug. Des. Discov.* **17,** 105–114
2. Civelli, O. (2005) *Trends Pharmacol. Sci.* **26,** 15–19

3. Wise, A., Jupe, S. C., and Rees, S. (2004) *Annu. Rev. Pharmacol. Toxicol.* **44,** 43–66
4. Oh, D. Y., Kim, K., Kwon, H. B., and Seong, J. Y. (2006) *Int. Rev. Cytol.* **252,** 163–218
5. Lee, D. K., Nguyen, T., Lynch, K. R., Cheng, R., Vanti, W. B., Arkhitko, O., Lewis, T., Evans, J. F., George, S. R., and O'Dowd, B. F. (2001) *Gene* (*Amst.*) **275,** 83–91
6. Lee, C. W., Rivera, R., Gardell, S., Dubin, A. E., and Chun, J. (2006) *J. Biol. Chem.* **281,** 23589–23597
7. Noguchi, K., Ishii, S., and Shimizu, T. (2003) *J. Biol. Chem.* **278,** 25600–25606
8. Kotarsky, K., Boketoft, A., Bristulf, J., Nilsson, N. E., Norberg, A., Hansson, S., Owman, C., Sillard, R., Leeb-Lundberg, L. M., and Olde, B. (2006) *J. Pharmacol. Exp. Ther.* **318,** 619–628
9. Choi, S., Lee, M., Shiu, A. L., Yo, S. J., Hallden, G., and Aponte, G. W. (2007) *Am. J. Physiol.* **292,** G1366–G1375
10. Huang, S. M., Bisogno, T., Petros, T. J., Chang, S. Y., Zavitsanos, P. A., Zipkin, R. E., Sivakumar, R., Coop, A., Maeda, D. Y., De Petrocellis, L., Burstein, S., Di Marzo, V., and Walker, J. M. (2001) *J. Biol. Chem.* **276,** 42639–42644
11. Acharjee, S., Do-Rego, J. L., Oh, D. Y., Ahn, R. S., Choe, H., Vaudry, H., Kim, K., Seong, J. Y., and Kwon, H. B. (2004) *J. Biol. Chem.* **279,** 54445–54453
12. Fumagalli, M., Trincavelli, L., Lecca, D., Martini, C., Ciana, P., and Abbracchio, M. P. (2004) *Biochem. Pharmacol.* **68,** 113–124
13. Oh, D. Y., Song, J. A., Moon, J. S., Moon, M. J., Kim, J. I., Kim, K., Kwon, H. B., and Seong, J. Y. (2005) *Mol. Endocrinol.* **19,** 722–731
14. Okada, T., Sugihara, M., Bondar, A. N., Elstner, M., Entel, P., and Buss, V. (2004) *J. Mol. Biol.* **342,** 571–583
15. Canutescu, A. A., and Dunbrack, R. L., Jr. (2005) *Bioinformatics* **21,** 2914–2916
16. Verdonk, M. L., Cole, J. C., Hartshorn, M. J., Murray, C. W., and Taylor, R. D. (2003) *Proteins* **52,** 609–623
17. Rhim, H., Kim, H., Lee, D. Y., Oh, T. H., and Nah, S. Y. (2002) *Eur. J. Pharmacol.* **436,** 151–158
18. Konstantinopoulos, P. A., Karamouzis, M. V., and Papavassiliou, A. G. (2007) *Nat. Rev. Drug. Discov.* **6,** 541–555
19. Akgoz, M., Kalyanaraman, V., and Gautam, N. (2006) *Cell. Signal.* **18,** 1758–1768
20. Taylor, J. S., Reid, T. S., Terry, K. L., Casey, P. J., and Beese, L. S. (2003) *EMBO J.* **22,** 5963–5974
21. Das, S., Schapira, M., Tomic-Canic, M., Goyanka, R., Cardozo, T., and Samuels, H. H. (2007) *Mol. Endocrinol.* **21,** 2672–2686
22. Saisho, Y., Morimoto, A., and Umeda, T. (1997) *Anal. Biochem.* **252,** 89–95
23. Kohno, M., Hasegawa, H., Inoue, A., Muraoka, M., Miyazaki, T., Oka, K., and Yasukawa, M. (2006) *Biochem. Biophys. Res. Commun.* **347,** 827–832
24. Gantz, I., Muraoka, A., Yang, Y. K., Samuelson, L. C., Zimmerman, E. M., Cook, H., and Yamada, T. (1997) *Genomics* **42,** 462–466
25. Vassilatis, D. K., Hohmann, J. G., Zeng, H., Li, F., Ranchalis, J. E., Mortrud, M. T., Brown, A., Rodriguez, S. S., Weller, J. R., Wright, A. C., Bergmann, J. E., and Gaitanaris, G. A. (2003) *Proc. Natl. Acad. Sci. U. S. A.* **100,** 4903–4908
26. Runquist, M., Parmryd, I., Thelin, A., Chojnacki, T., and Dallner, G. (1995) *J. Neurochem.* **65,** 2299–2306
27. Caterina, M. J., Rosen, T. A., Tominaga, M., Brake, A. J., and Julius, D. (1999) *Nature* **398,** 436–441
28. Kinloch, R. A., and Cox, P. J. (2005) *Expert Opin. Ther. Targets* **9,** 685–698
29. Succar, R., Mitchell, V. A., and Vaughan, C. W. (2007) *Mol. Pain* **3,** 24
30. Vuong, L. A., Mitchell, V. A., and Vaughan, C. W. (2008) *Neuropharmacology* **54,** 189–193
31. Sheskin, T., Hanus, L., Slager, J., Vogel, Z., and Mechoulam, R. (1997) *J. Med. Chem.* **40,** 659–667
32. Devane, W. A., Hanus, L., Breuer, A., Pertwee, R. G., Stevenson, L. A., Griffin, G., Gibson, D., Mandelbaum, A., Etinger, A., and Mechoulam, R. (1992) *Science* **258,** 1946–1949
33. Burstein, S. H., Huang, S. M., Petros, T. J., Rossetti, R. G., Walker, J. M., and Zurier, R. B. (2002) *Biochem. Pharmacol.* **64,** 1147–1150